Propagation of Equatorially Trapped Waves on a Sloping Thermocline

JIAYAN YANG AND LISAN YU*

Mesoscale Air–Sea Interaction Group, Florida State University, Tallahassee, Florida

(Manuscript received 6 August 1990, in final form 19 July 1991)

ABSTRACT

The WKBJ method and a multiple-scale expansion technique are used to study equatorially trapped waves propagating on a zonally sloping thermocline. Assuming that variations of the main thermocline depth (MTD) are slow (the change of the MTD over one wavelength is smaller than the wave amplitude), wave reflections can be neglected and the amplitudes of equatorially trapped waves can be derived by using the energy conservation law. It is found that the wavelengths and amplitudes of free waves are significantly modified by the MTD variations. While propagating eastward in an ocean basin (where the MTD is shallower), Kelvin waves shrink meridionally and zonally but their amplitudes increase to preserve wave energy; short Rossby waves behave in the opposite way. The wavelength of westward-propagating long Rossby waves becomes longer when they propagate into the deeper western ocean. The response of a Yanai wave to the changing thermocline depends on the sign of phase speed.

A simple numerical method is designed to verify the WKBJ results and also to study the case of a relatively steep thermocline profile where the WKBJ method breaks down. Reflection of a Kelvin wave impinging on a thermocline front is also investigated in this work.

1. Introduction

Oceanic variability in the tropical oceans has been studied extensively over the past two decades, especially those low-frequency interannual phenomena associated with El Niño–Southern Oscillation (ENSO) (e.g., Hurlburt et al. 1976; McCreary 1976; Battisti and Hirst 1989). However, in most analytical models the horizontal variations of the density field are ignored and the density is assumed to be a function of depth only. A striking feature of the equatorial ocean thermal structure is that the SST increases westward, and the main thermocline, which separates warm surface water from colder deep water, is shoaling eastward. For example, in the Pacific Ocean, the isotherm of 20°C water rises from 175 m at 160°E to about 75 m at 100°W (Colin et al. 1971). A similar feature is also observed in the equatorial Atlantic Ocean (Merle 1980).

An eastward-tilted thermocline has an important influence on both the dynamics and thermodynamics of coupled atmosphere–ocean models. For example, the greater subsurface vertical temperature gradient associated with the shallower main thermocline in the eastern Pacific is critical to localize the SST anomalies associated with coupled instabilities, while a deep thermocline in the western Pacific Ocean enables Rossby waves to propagate freely westward. These two effects, together with the reflectibility of the western boundary, constitute the so-called "delayed action oscillator" discovered by Suarez and Schopf (1989) and Battisti and Hirst (1989).

The effects of a zonally sloping thermocline on equatorially trapped waves have been investigated by several researchers after Hughes (1981, hereafter H81). Gill and King (1985, hereafter GK85) used a two-layer reduced-gravity model to study the energy exchanges between two baroclinic modes when a Kelvin wave propagates through a tilted thermocline, Busalacchi and Cane (1988) have shown that equatorially trapped waves will be reflected from a density discontinuity front by using the method of island reflections similar to that of Cane and du Penhoat (1981). More recently, Long and Chang (1990, hereafter LC90) have studied the nonlinearity of a Kelvin wave front propagating on a sloping thermocline. In LC90, it was shown that the nonlinear evolution of a Kelvin wave is governed by the perturbed KdV equation. Weak meridional variations of the main thermocline depth (MTD) are also included in LC90. Also, LC90 studied the conservation of both mass and energy in the case of a nonperiodic Kelvin wave front.

In this paper, we will use the WKBJ method and the condition of energy conservation to derive all types of linear wave solutions in a background of a sloping thermocline (section 2). All waves are assumed to be periodic and that they do not carry mass, the condition

* Also affiliated with Supercomputer Computations Research Institute, Florida State University, Tallahassee, FL 32306.

Corresponding author address: Dr. Jiayan Yang, Mesoscale Air–Sea Interaction Group, Florida State University, M.S.B-174, Love 012, Tallahassee, FL 32306-3041.

of mass conservation is satisfied. The method is similar to that of H81, but the results show some differences. Our solution for Kelvin waves agrees with that of H81 completely. However, Rossby waves, Yanai waves, and inertia–gravity waves differ greatly from H81. The differences between H81 and our solution come from the condition (8), that is, $h \propto H^{1/2}u \propto H^{1/2}v$, used in H81. This condition is not valid for Rossby waves, Yanai waves, and inertial–gravity waves. In section 3, we design a simple reduced-gravity baroclinic model to verify our analytical results and to test wave propagations on a relatively steep thermocline where the WKBJ method does not work. A conclusion is given in section 4.

2. Effects of a slowly varying thermocline: WKBJ solutions

We assume, in the following discussion, that the MTD changes slowly in longitude so that wave reflections are negligible; that is, the sloping thermocline is not an effective barrier for wave propagations. For a faster varying MTD, a propagating wave is continually scattered and a solution to such waves can only be found numerically. The sloping thermocline is assumed to be maintained by easterly trade winds (GK85; H81) although oceanic waves also contribute to some local variabilities of the main thermocline. Since this work is to investigate the effects of the existing nonuniform climatological conditions on trapped waves, the effects of local thermocline variability caused by waves are excluded.

The mean depth of the thermocline H_0 is assumed as

$$H_0 = D_0 + d(\epsilon x) \quad \text{for} \quad 0 < x < L, \tag{2.1}$$

where x is the zonal coordinate with positive direction eastward, L is the basin width, D_0 is the thermocline depth at the western boundary, $d(\epsilon x)$ is the deviation of the MTD from its value at $x = 0$, and ϵ is a small parameter such that

$$\epsilon \sim \frac{dH_0}{dx} \ll [k_0\eta_0]^{-1}. \tag{2.2}$$

The parameters k_0 and η_0 represent the zonally averaged wavenumber and wave amplitude, respectively. We assume (2.2) is satisfied in the following derivation, while we are aware that this assumption may be violated for a very long wave.

The linear, inviscid, free wave equations are used in a $1\frac{1}{2}$-layer ocean model; that is,

$$\frac{\partial u}{\partial t} - \beta y v = -g'\frac{\partial h}{\partial x} \tag{2.3a}$$

$$\frac{\partial v}{\partial t} + \beta y u = -g'\frac{\partial h}{\partial y} \tag{2.3b}$$

$$\frac{\partial h}{\partial t} + \frac{\partial}{\partial x}[H_0(\epsilon x)u] + \frac{\partial}{\partial y}[H_0(\epsilon x)v] = 0. \tag{2.3c}$$

The variable h is the departure of the upper-layer thickness from its mean state $H_0(\epsilon x)$. Zonal velocity is denoted by u, meridional velocity by v, and g' is the reduced gravity.

There are several types of waves existing in an equatorial waveguide, such as Kelvin waves, Rossby waves, high-frequency inertia–gravity waves, and Yanai waves. The responses of each type of wave to the sloping thermocline will be discussed separately.

a. Kelvin wave ($v = 0$)

An equatorially trapped Kelvin wave is a nondispersive gravity wave traveling eastward with zero meridional velocity. It is assumed that

$$(u, h) = (\tilde{u}, \tilde{h}) \exp(-i\omega t) \tag{2.4}$$

where $\tilde{u}$, $\tilde{h}$ are to be determined. Let $v = 0$; (2.3a) and (2.3c) can be reduced to an equation for $\tilde{h}$:

$$\frac{\partial}{\partial \tau}\left[H_0(\tau)\frac{\partial \tilde{h}}{\partial \tau}\right] + \frac{\omega^2}{\epsilon^2 g'}\tilde{h} = 0 \tag{2.5}$$

where $\tau = \epsilon x$ is introduced as a slow variable.

The second-order differential equation (2.5) is a well-known Sturm–Liouville equation. To solve this kind of equation, it is standard to define a fast variable:

$$\xi = \frac{1}{\epsilon}\int_0^\tau \omega(g'H_0(\tau))^{-1/2}d\tau.$$

In terms of the variables ξ and τ, Eq. (2.5) becomes

$$\frac{\partial^2 \tilde{h}}{\partial \xi^2} + \frac{\epsilon}{2\omega H_0}(g'H_0)^{1/2}\frac{dH_0(\tau)}{d\tau}\frac{\partial \tilde{h}}{\partial \xi} + \tilde{h} = 0 \tag{2.6}$$

which now can be solved by using the two-variable expansion method. Let

$$\tilde{h} = \tilde{h}_0(\xi, \tau, y) + \epsilon\tilde{h}_1(\xi, \tau, y) + O(\epsilon^2); \tag{2.7}$$

the lowest order of the expansion yields

$$\frac{\partial^2 \tilde{h}_0}{\partial \xi^2} + \tilde{h}_0 = 0$$

which is an equation for the fast variable ξ alone and has a solution of the form:

$$\tilde{h}_0(\xi, \tau) = A_0(\tau, y)\exp\{i\xi(\tau)\} \tag{2.8}$$

where A_0 is the undetermined wave amplitude.

The wave phase is given by (2.4) and (2.8); that is, $Q(\tau, t) = \xi(\tau) - \omega t$. The wavenumber is then

$$k(\tau) = \frac{\partial}{\partial x}Q(\tau, t) = \omega(g'H_0(\tau))^{-1/2}. \tag{2.9}$$

If $\epsilon = 0$, that is, the thermocline is flat, then k

$= \omega(g'D_0)^{-1/2}$. So, we recover the nondispersive Kelvin-wave solution in a homogeneous background.

Eliminating u between Eqs. (2.3b) and (2.3c) after letting $v = 0$, and applying (2.7)–(2.9), to the lowest order, yields

$$(g'H_0(\tau))^{-1/2}\beta y A_0 + \frac{\partial A_0}{\partial y} = 0. \qquad (2.10)$$

The solution of (2.10) is $A_0 = P_0(\tau)\exp[-y^2/(2\lambda(\tau)^2)]$, where $\lambda(\tau) = \sqrt{c(\tau)/\beta}$ is the local Rossby deformation radius, varying with x; P_0 can be calculated by the energy conservation constraint.

The total energy of a Kelvin wave is expressed as

$$E_k = \frac{1}{2}\frac{\omega}{2\pi}\int_{-\infty}^{+\infty}\int_{x-0.5L_k}^{x+0.5L_k}\int_{t-\pi/\omega}^{t+\pi/\omega}[H_0u^2 + g'h^2]dtdxdy$$

where $L_k(\tau) = 2\pi/k(\tau) = 2\pi\omega^{-1}(g'H_0(\tau))^{1/2}$ is the local wavelength. Based on the local WKBJ approximation, $P_0(\tau)$, $L_k(\tau)$, and $\lambda(\tau)$ are constant locally. Therefore, we have

$$E_k = \text{const} \times \lambda(\tau)L_k(\tau)P_0(\tau)^2.$$

Since we have assumed that the energy scattering is negligible, the total energy is conserved to $O(\epsilon)$; that is, E_k is a constant. Then, P_0 is obtained:

$$P_0(\tau) = C_0H_0(\tau)^{-3/8}$$

where C_0 is a constant determined by the initial condition of wave field. Finally, the solution for the Kelvin wave is obtained; that is,

$$h = C_0H_0(\tau)^{-3/8}\exp\left(-\frac{y^2}{2\lambda(\tau)^2}\right) \times \exp\{i\xi(\tau) - i\omega t\} + O(\epsilon) \qquad (2.11a)$$

$$u = C_0\sqrt{g'}H_0(\tau)^{-7/8}\exp\left(-\frac{y^2}{2\lambda(\tau)^2}\right) \times \exp\{i\xi(\tau) - i\omega t\} + O(\epsilon). \qquad (2.11b)$$

Equation (2.11) agrees completely with H81.

b. Other equatorially trapped waves

Defining transport velocities as $(U, V) = H_0(u, v)$, (2.3a)–(2.3c) take the form:

$$\frac{\partial U}{\partial t} - \beta yV = -[c(\epsilon x)]^2\frac{\partial h}{\partial x} \qquad (2.12a)$$

$$\frac{\partial V}{\partial t} + \beta yU = -[c(\epsilon x)]^2\frac{\partial h}{\partial y} \qquad (2.12b)$$

$$\frac{\partial h}{\partial t} + \frac{\partial U}{\partial x} + \frac{\partial V}{\partial y} = 0 \qquad (2.12c)$$

where $c(\epsilon x) = (g'H_0(\epsilon x))^{1/2}$ is the modified gravity wave speed.

Eliminating h and U from (2.12a)–(2.12c), a single equation of V is then derived:

$$\frac{\partial}{\partial t}\left\{\frac{1}{c(\epsilon x)^2}\frac{\partial^2}{\partial t^2} + \frac{\partial^2}{\partial x^2} + \frac{\partial^2}{\partial y^2} - \beta^2y^2\right\}V - \beta\frac{\partial V}{\partial x} = 0. \qquad (2.13)$$

Since the wave phase changes much faster than the zonal background, we may define a general wave solution as

$$V = A_v(\tau, y)\exp(i\theta(\tau)/\epsilon - i\omega t). \qquad (2.14)$$

Again, $\tau = \epsilon x$ is a slow variable.

Substituting (2.14) to (2.13) yields an equation to leading order:

$$\frac{\partial^2 A_v}{\partial y^2} - \left[\frac{(\beta^2y^2 - \omega^2)}{c(\tau)^2} + \left(\frac{d\theta}{d\tau}\right)^2 + \frac{\beta}{\omega}\frac{d\theta}{d\tau}\right]A_v = O(\epsilon). \qquad (2.15)$$

This is the parabolic cylinder equation that has been discussed extensively by Moore (1968) and Moore and Philander (1977). It has a set of bounded solutions only when

$$\frac{c(\tau)}{\beta}\left[\frac{\omega^2}{c(\tau)^2} - \left(\frac{d\theta_n}{d\tau}\right)^2 - \frac{\beta}{\omega}\frac{d\theta_n}{d\tau}\right] = 2n + 1 \qquad (2.16)$$

where n is a positive integer or zero (Yanai wave). This is the dispersion relation of equatorially trapped waves with slowly varying state. It implies that the right-hand side of (2.16) must be τ independent and equals a positive odd integer. Under this condition, the unknown function $d\theta_n/d\tau$ is related to the known gravity wave speed $c(\tau)$. Or in other words, $d\theta_n/d\tau$ must adjust itself to make the right-hand side of (2.16) a positive odd integer in order to have a meridionally bounded solution.

For a wave phase $Q(\epsilon x, t) = \theta_n(\epsilon x)/\epsilon - \omega t$ given by (2.14), the wavenumber is

$$k_n(\tau) = \frac{\partial}{\partial x}Q(\epsilon x, t) = \frac{d\theta_n}{d\tau}$$

and can be calculated from (2.16),

$$\frac{d\theta_n}{d\tau} = \frac{1}{2}\left\{-\frac{\beta}{\omega} \pm \left[\left(\frac{\beta}{\omega}\right)^2 - \frac{4(2n+1)\beta}{c(\tau)} + 4\left(\frac{\omega}{c(\tau)}\right)^2\right]^{1/2}\right\}. \qquad (2.17)$$

Integration of (2.17) yields

$$\theta_n(\tau) = \int_0^\tau k_n(\tau)d\tau = \int_0^\tau \frac{1}{2}\left\{-\frac{\beta}{\omega} \pm \left[\left(\frac{\beta}{\omega}\right)^2 - \frac{4(2n+1)\beta}{c(\tau)} + 4\left(\frac{\omega}{c(\tau)}\right)^2\right]^{1/2}\right\}d\tau. \qquad (2.18)$$

The bounded solution of (2.15) is $A_{vn}(\tau, y) = P_n(\tau)D_n(y/\lambda(\tau))$, where D_n is the Hermite function, $\lambda(\tau) = (c(\tau)/\beta)^{1/2}$ is the local Rossby deformation radius, and $P_n(\tau)$ is the wave amplitude. Thus, the meridional transport velocity V governed by (2.13) takes the form:

$$V_n(x, y, t) = P_n(\tau)D_n\left(\frac{y}{\lambda(\tau)}\right)\exp(i\theta_n(\tau)/\epsilon - i\omega t). \quad (2.19)$$

With the aid of the recurrence relations of Hermite functions, we can derive the zonal transport velocity U and the pressure field h:

$$U_n = A_{un}(\tau, y)\exp(i\theta_n(\tau)/\epsilon - i\omega t) \quad (2.20)$$

$$h_n = A_{hn}(\tau, y)\exp(i\theta_n(\tau)/\epsilon - i\omega t) \quad (2.21)$$

where

$$A_{un}(\tau, y) = i\left(\frac{\beta c(\tau)}{2}\right)^{1/2}P_n(\tau)\left[\frac{\sqrt{n+1}}{\omega - c(\tau)k_n(\tau)} \times D_{n+1}\left(\frac{y}{\lambda}\right) + \frac{\sqrt{n}}{\omega + c(\tau)k_n(\tau)}D_{n-1}\left(\frac{y}{\lambda}\right)\right]$$

$$A_{hn}(\tau, y) = i\left(\frac{\beta}{2c(\tau)}\right)^{1/2}P_n(\tau)\left[\frac{\sqrt{n+1}}{\omega - c(\tau)k_n(\tau)} \times D_{n+1}\left(\frac{y}{\lambda}\right) - \frac{\sqrt{n}}{\omega + c(\tau)k_n(\tau)}D_{n-1}\left(\frac{y}{\lambda}\right)\right].$$

To determine the amplitude $P_n(\tau)$, the energy conservation condition is used. The total wave energy averaged over one wave period is defined as

$$E = \frac{1}{2}\frac{\omega}{2\pi}\int_{-\infty}^{+\infty}\int_{x-0.5L}^{x+0.5L}\int_{t-\pi/\omega}^{t+\pi/\omega}\left[\frac{U^2+V^2}{H_0} + g'h^2\right]dtdxdy \quad (2.22)$$

where $L = 2\pi[d\theta/d\tau]^{-1}$ is the local wavelength. Since the normalized Hermite functions $D_n(z)$ satisfies

$$\int_{-\infty}^{+\infty}D_n(z)D_m(z)dz = \delta_{nm}$$

$$(=1, \text{ if } m = n; = 0 \text{ otherwise}).$$

Equation (2.22) results in

$$E_n = \frac{1}{4}P_n(\tau)\chi_n(\tau)^2 \quad (2.23)$$

where

$$\chi_n(\tau)^2 = \frac{L(\tau)\lambda(\tau)}{H_0(\tau)}\left\{1 + \beta c(\tau)\left[\frac{n+1}{(\omega - c(\tau)k(\tau))^2} + \frac{n}{(\omega + c(\tau)k(\tau))^2}\right]\right\}. \quad (2.24)$$

The energy conservation constraint thus gives

$$P_n(\tau) = c_0\chi_n(\tau)^{-1} \quad (2.25)$$

where c_0 is a constant.

Equations (2.19)–(2.21) are the general solutions of equatorially trapped Rossby, Yanai, and inertial-gravity waves. They do not agree with the condition (8) of H81. This disagreement leads to our different conclusions. To show that more explicitly, we shall discuss several wave solutions.

For a long Rossby wave with a dispersion relation $\omega = -ck/(2n+1)$, (2.24) can be simplified to

$$\chi_n(\tau)^2 = \frac{L(\tau)\lambda(\tau)}{H_0(\tau)}\left[1 + \frac{(2n+1)\beta c(\tau)}{4\omega^2 n(n+1)}\right].$$

For low-frequency waves, that is, $\omega \ll \sqrt{\beta c}$, it can be further simplified to

$$\chi_n(\tau)^2 = a_0 H(\tau)^{1/4} \quad (2.26)$$

where a_0 is a τ-independent constant.

With (2.25) and (2.26), a low-frequency long Rossby wave solution can be written as

$$u = iH_0(\tau)^{-1}C_0\left(\frac{\beta\sqrt{g'}}{2}\right)^{1/2} \times \left[\frac{1}{2\omega\sqrt{2n+1}}D_{n+1}\left(\frac{y}{\lambda}\right) - \frac{1}{2\omega\sqrt{n}}D_{n-1}\left(\frac{y}{\lambda}\right)\right] \times \exp(i\theta_n(\tau)/\epsilon - i\omega t) \quad (2.27a)$$

$$v = C_0H_0(\tau)^{-9/8}D_n\left(\frac{y}{\lambda(\tau)}\right) \times \exp(i\theta_n(\tau)/\epsilon - i\omega t) \quad (2.27b)$$

$$h = iH_0(\tau)^{-3/8}C_0\left(\frac{\beta}{2\sqrt{g'}}\right)^{1/2} \times \left[\frac{1}{2\omega\sqrt{2n+1}}D_{n+1}\left(\frac{y}{\lambda}\right) + \frac{1}{2\omega\sqrt{n}}D_{n-1}\left(\frac{y}{\lambda}\right)\right] \times \exp(i\theta_n(\tau)/\epsilon - i\omega t). \quad (2.27c)$$

The Yanai wave is another type of trapped wave that only exists in the equatorial waveguide. If $n = 0$ in (2.16), we obtain the dispersion relation of Yanai waves:

$$k = \frac{\omega}{c} - \frac{\beta}{\omega}. \quad (2.28)$$

A solution for the Yanai wave is [from (2.19)–(2.21) and (2.28) with $n = 0$]

$$V_0 = P_0(\tau)\exp[-y^2\lambda(\tau)^{-2}2^{-1}] \times \exp\left\{i\left(\frac{\omega}{c} - \frac{\beta}{\omega}\right)x - i\omega t\right\}. \quad (2.29a)$$

The corresponding u and h fields are

$$U_0 = i\omega(2\beta c)^{-1/2}P_0(\tau)D_1\left(\frac{y}{\lambda}\right) \times \exp\left\{i\left(\frac{\omega}{c}-\frac{\beta}{\omega}\right)x - i\omega t\right\} \quad (2.29b)$$

$$h_0 = i\omega c^{-1}(2\beta c)^{-1/2}P_0(\tau)D_1\left(\frac{y}{\lambda}\right) \times \exp\left\{i\left(\frac{\omega}{c}-\frac{\beta}{\omega}\right)x - i\omega t\right\}. \quad (2.29c)$$

By taking $n = 0$ and using the dispersion relation (2.28), (2.24) becomes

$$\chi_0(\tau)^2 = \frac{L_0(\tau)\lambda(\tau)}{H_0(\tau)}\left[1 + \frac{\omega^2}{\beta c(\tau)}\right]$$

where the wavelength is

$$L_0 = \frac{2\pi}{|k|} = \frac{2\pi\beta c(\tau)}{|(\omega^2 - \beta c(\tau))|}. \quad (2.30)$$

Therefore,

$$\chi_0(\tau)^2 = \text{const} \times \left[\frac{\omega^2 + \beta c(\tau)}{|\omega^2 - \beta c(\tau)|}\right]H_0(\tau)^{-3/4}$$

and

$$P_0(\tau) = \text{const} \times \left[\frac{|\omega^2 - \beta c(\tau)|}{\omega^2 + \beta c(\tau)}\right]^{1/2} H_0(\tau)^{3/8}.$$

The Yanai wave solution is then derived:

$$u = H_0^{-1}U_0 = i\omega a_0(2\beta)^{-1/2}g'^{-1/4}\left[\frac{|\omega^2 - \beta c(\tau)|}{\omega^2 + \beta c(\tau)}\right]^{1/2} \times H_0(\tau)^{-7/8}D_1\left(\frac{y}{\lambda}\right) \times \exp\left\{i\left(\frac{\omega}{c}-\frac{\beta}{\omega}\right)x - i\omega t\right\} \quad (2.31a)$$

$$v = \mathrm{H}_0^{-1}\mathrm{V}_0 = \mathrm{a}_0\left[\frac{|\omega^2 - \beta\mathrm{c}(\tau)|}{\omega^2 + \beta\mathrm{c}(\tau)}\right]^{1/2} \times H_0(\tau)^{-5/8}\exp[-y^2\lambda(\tau)^{-2}2^{-1}] \times \exp\left\{i\left(\frac{\omega}{c}-\frac{\beta}{\omega}\right)x - i\omega t\right\} \quad (2.31b)$$

$$h = i\omega a_0(2\beta)^{-1/2}g'^{-3/4}\left[\frac{|\omega^2 - \beta c(\tau)|}{\omega^2 + \beta c(\tau)}\right]^{1/2} \times H_0(\tau)^{-3/8}D_1\left(\frac{y}{\lambda}\right) \times \exp\left\{i\left(\frac{\omega}{c}-\frac{\beta}{\omega}\right)x - i\omega t\right\}. \quad (2.31c)$$

In the high-frequency limit, the dispersion relation (2.16) is simplified to

$$[k(\tau)]^2 = \left(\frac{\omega}{c}\right)^2 - \frac{(2n+1)\beta}{c}. \quad (2.32)$$

Equation (2.32) is the dispersion relation for the high-frequency inertial–gravity waves trapped by the equator. Solutions of inertial–gravity waves can be easily obtained from (2.19), (2.20), (2.21), (2.24), (2.25), and (2.32) in a way similar to these discussions.

3. Discussion of WKBJ results

In the previous section we have derived the leading-order solutions to the equatorially trapped waves in the case where the main thermocline slowly tilts in longitude. In this section, some detailed discussions and interpretations are given to those wave solutions.

The wavelength of a Kelvin wave propagating on a sloping thermocline is determined by (2.9); that is,

$$L_K(\epsilon x) = \frac{2\pi}{k(\epsilon x)} = 2\pi g'\omega^{-1}H_0(\epsilon x)^{1/2} \quad (3.1)$$

and ULHA (the upper-layer thickness anomaly) is given by (2.11):

$$h \sim H_0(\epsilon x)^{-3/8}. \quad (3.2)$$

Clearly from (3.1), the shallower the thermocline, the shorter the wavelength will be. The wave amplitude behaves in the opposite way, as exhibited by (3.2). There are two factors contributing to the change of wave amplitude h. One is due to the shortening zonal wavelength as predicted by (3.1); the other is attributed to the reduced meridional trapping scale.

Another important effect of a sloping thermocline is to delay the signals of remote forcing; that is, decelerating Kelvin waves take a longer time to transmit the wind input energy from the west to the central and eastern tropical oceans. To show that, let us assume the main thermocline depth is linearly tilted in longitude; that is, $H_0(x) = D_0 - \delta x$, where x is the distance from the center of wind forcing at time t. Hence, we have $dx/dt = c(\epsilon x) = \sqrt{g'(D_0 - \delta x)}$. An integration of time t yields the $x - t$ relationship:

$$x(t) = \sqrt{g'D_0}t - \frac{\delta g'}{4}t^2. \quad (3.3)$$

The $x(t) - t$ relation (3.3) is plotted in Fig. 1 for some chosen parameters; that is, $g' = 0.02$ and δ from 0 to 1.2×10^{-5}. It shows that it takes only 65 days for a Kelvin wave to travel across a basin of width 12 000 km in a flat thermocline of depth D_0, while it would take 150 days to propagate over the same distance if the thermocline slope is $\delta = 1.2 \times 10^{-5}$.

This implies that for a model with a flat thermocline of 200 m in depth, three months will be enough for a

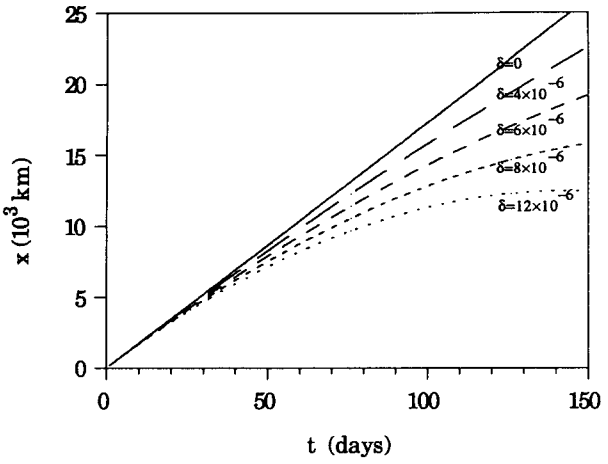

FIG. 1. Plot of $x(t)$ of Eq. (3.3) for different thermocline slope.

baroclinic Kelvin wave to travel across the Pacific Ocean and less than nine months (the first-mode long Rossby wave propagates with one-third of the Kelvin wave speed) will be taken for the fastest reflected long Rossby waves to travel back to the western Pacific Ocean. However, in a modest sloping thermocline, for example, $\delta = 0.8$–$1.2(\times 10^{-5})$, it will take at least two years to complete this same cycle. This effect may be important in the adjusting time scale of the model. At least we should consider the effect of a sloping thermocline in the El Niño prediction models in order to improve accuracy.

The dispersion relation for low-frequency Rossby waves given by (2.16) is

$$k_n(\epsilon x) = \frac{1}{2}\left\{-\frac{\beta}{\omega} \pm \left[\left(\frac{\beta}{\omega}\right)^2 - \frac{4(2n+1)\beta}{c(\epsilon x)}\right]^{1/2}\right\} \quad (3.4)$$

where the upper sign is for long Rossby waves and the lower sign is for short Rossby waves. The wavelength of a long Rossby wave is

$$L_n^l(\epsilon x) = 4\pi\left\{\frac{\beta}{\omega} - \left[\left(\frac{\beta}{\omega}\right)^2 - \frac{4(2n+1)\beta}{c(\epsilon x)}\right]^{1/2}\right\}^{-1}. \quad (3.5)$$

For low-frequency waves such that $\omega^2 \ll \beta c$, (3.5) is approximated as $L_n^l(\epsilon x) = 2\pi c(\epsilon x)/[(2n+1)\omega] \sim H_0(\epsilon x)^{1/2}$, which is the same as that of Kelvin waves. The wavelength of a short Rossby wave is determined by

$$L_n^s(\epsilon x) = 4\pi\left\{\frac{\beta}{\omega} + \left[\left(\frac{\beta}{\omega}\right)^2 - \frac{4(2n+1)\beta}{c(\epsilon x)}\right]^{1/2}\right\}^{-1}. \quad (3.6)$$

If the main thermocline is shoaling eastward; that is, $dH_0/dx \leqslant 0$, a short Rossby wave will become longer in the eastern oceans because $dL_n^s(\epsilon x)/dx \geqslant 0$.

Obviously, the response of a long Rossby wave traveling in a sloping thermocline is similar to that of a Kelvin wave; that is, its amplitude decreases westward to conserve the total energy as its wavelength increases. For a short Rossby wave, an opposite scenario is seen.

As one notes, the only longitudinal dependent term in (3.5) and (3.6) is $4(2n+1)\beta/c(\epsilon x)$. It is not surprising that the variations of the MTD have greater effect on the higher-mode Rossby waves. It is also found that the lower-frequency Rossby waves are less sensitive to the MTD changes because the first term inside the square root, $(\beta/\omega)^2$, is dominant over the term associated with the thermocline change, that is, $4(2n+1)\beta/c(\epsilon x)$.

Amplified Kelvin and long Rossby waves at the central and eastern tropical oceans not only induce greater SST anomalies by strengthening upwelling–downwelling processes, but also enhance the role of advection in the local thermodynamics. McPhaden and Picaut (1990) have shown that the eastward advections associated with remotely generated Rossby waves play an important role in the scenario of El Niño phenomena in the western Pacific. From (2.11) and (2.27), we have

$$u_{\text{Kelvin}} \sim H_0(\epsilon x)^{-7/8} \quad (3.7a)$$

$$u_{\text{Rossby}} \sim H_0(\epsilon x)^{-1} \quad (3.7b)$$

$$v_{\text{Rossby}} \sim H_0(\epsilon x)^{-9/8}. \quad (3.7c)$$

For a Kelvin wave traveling from a position with $H_0 = 200$ m to where $H_0 = 100$ m, its induced velocity increases 83.4%. Long Rossby waves have even greater responses to such changes; for example, u_{Rossby} and v_{Rossby} would increase 100% and 118%, respectively. Such dramatic changes in wave-induced motion make advection processes more effective in the central and eastern oceans where the main thermocline jumps from 150 m to less than 50 m and the SST experiences the greatest zonal gradient.

A Yanai wave is an antisymmetrical wave that exists only in the equatorial waveguide. In the lower-frequency range ($\omega < \sqrt{c(\epsilon x)\beta}$), it behaves like a short Rossby wave with eastward group velocity and westward phase speed. For a higher-frequency wave ($\omega \geqslant \sqrt{c(\epsilon x)\beta}$), it acts as a Kelvin wave with eastward group and phase velocities.

It is interesting to note that the sign of the Yanai wave phase speed changes when the thermocline depth changes. From the dispersion relation (2.28), the frequency of a Yanai wave at $k \approx 0$ (infinite long wave) is $\omega = \sqrt{c(\epsilon x)\beta}$. For a long Yanai wave with frequency $\omega_0 = \sqrt{c(0)\beta}(1 - \epsilon_0)$, where ϵ_0 is a small parameter, its wavenumber at $x = 0$ is

$$k_0 = \left(\frac{\omega_0}{c(0)} - \frac{\beta}{\omega_0}\right) = -2\left(\frac{\beta}{c(0)}\right)^{1/2}\epsilon_0 < 0 \quad (3.8)$$

that is, the phase speed is westward at $x = 0$. When this wave propagates to $x = x_1$ with $c_1 = [g'H_0 - (\epsilon x_1)]^{1/2} < c(0)$, its wavenumber changes to

$$k_1 = \left(\frac{\omega_0}{c_1} - \frac{\beta}{\omega_0}\right) \geq 0, \text{ if } c_1 \leq c(0)(1 - \epsilon_0)^2. \quad (3.9)$$

That is to say, for a long Yanai wave with an initial westward phase speed the sign of its phase speed changes as it propagates into a shallower area.

The wavelength of a Yanai wave with positive phase speed is

$$L_p = 2\pi\left(\frac{\omega}{c(\epsilon x)} - \frac{\beta}{\omega}\right)^{-1} \quad (3.10)$$

and with negative phase speed is

$$L_n = 2\pi\left(\frac{\beta}{\omega} - \frac{\omega}{c(\epsilon x)}\right)^{-1}. \quad (3.11)$$

From (3.10) and (3.11), we can see that $dL_p/dx \leq 0$ and $dL_n/dx \geq 0$ if $dc(\epsilon x)/dx \leq 0$. Therefore, the wavelength of a Yanai wave with positive phase speed decreases, while the wavelength of a Yanai wave with negative phase speed increases.

4. The numerical experiments

In this section, we design a numerical model to test the results we have derived and to study the effects of a relatively steep thermocline where the WKBJ method breaks down. The model is the simplest possible baroclinic ocean model consisting of a dynamically active surface layer of density ρ above a motionless, infinitely deep layer of slightly higher density $\rho + \Delta\rho$.

The equations (2.3a)–(2.3c) are discretized into a staggered grid (Arakawa C grid). The resolutions are $\Delta x = 40$ km in longitude and $\Delta y = 15$ km in latitude. A leapfrog scheme is used for time integration with $\Delta t = 30$ min. A forward time-differencing scheme is employed every 99 time steps to avoid the computational mode.

The profiles of main thermoclines are defined as (3.1). We chose the basin width L_0 to be 1.6×10^4 km and the thermocline depth at the western boundary D_0 to be 200 m.

The first experiment tests the Kelvin wave propagation on a sloping thermocline. An analytical solution to the equatorially trapped Kelvin wave is specified as a western boundary condition from where it travels eastward; that is,

$$h(0, y, t) = \Delta h \sin[\omega t] \exp\left[-\frac{y^2}{2\lambda_0^2}\right] \quad (4.1)$$

$$u(0, y, t) = \frac{g'\Delta h}{c} \sin[\omega t] \exp\left[-\frac{y^2}{2\lambda_0^2}\right] \quad (4.2)$$

$$v(0, y, t) = 0 \quad (4.3)$$

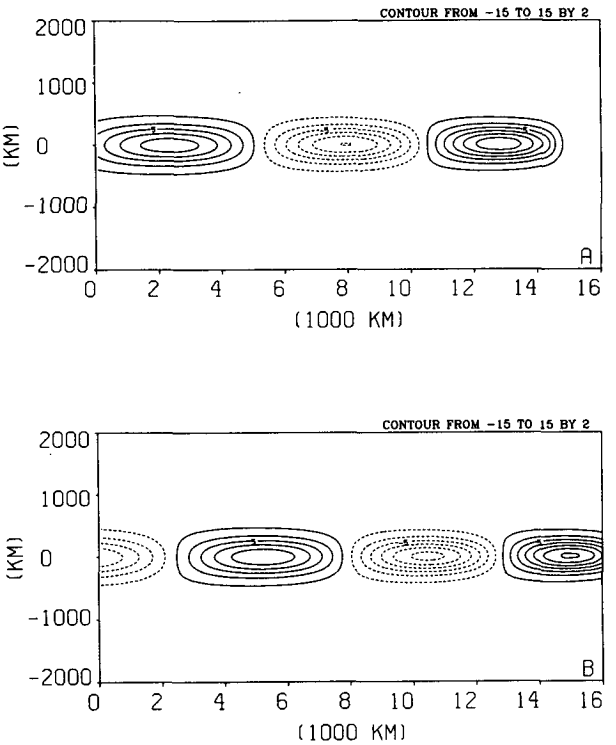

FIG. 2. Numerical simulations of Kelvin wave propagations at frequency $\omega = 2\pi/70$ days. (a) $\delta = 6.25 \times 10^{-6}$ at $t = 140$ days; (b) $\delta = 9.5 \times 10^{-6}$ at $t = 160$ days.

where Δh is the amplitude of the incoming Kelvin wave, $c = \sqrt{g'D_0}$ is the phase speed at $x = 0$, and $\lambda_0 = \sqrt{c/\beta}$ is the local Rossby deformation radius. The eastern boundary at $x = 1.6 \times 10^4$ km is open, and the method of Camerlengo and O'Brien (1980) is used to compute u, v, and h along the boundary. The advantage of using this method is that it allows the phenomena generated in the interior domain to pass through the open boundary without distortion and without affecting the interior solution.

In all the numerical tests the thermocline depth is linearly tilted; that is,

$$H_0(x) = 200 - \delta x. \quad (4.4)$$

Figure 2a shows the wave pattern at $t = 140$ days for $\delta = 6.25 \times 10^{-6}$ and $\omega = 2\pi/70$ days. It is easy to see that the wavelength becomes shortened and the amplitude is significantly enhanced as the Kelvin wave travels eastward. A more evident picture is given by Fig. 2b, where $\delta = 9.5 \times 10^{-6}$ and the contour is plotted at $t = 160$ days.

Next we use the same model to study the long Rossby wave propagation. Since a long Rossby wave travels westward, the western boundary is open now while the eastern boundary condition is specified by an analytical solution of the first-mode equatorially trapped Rossby

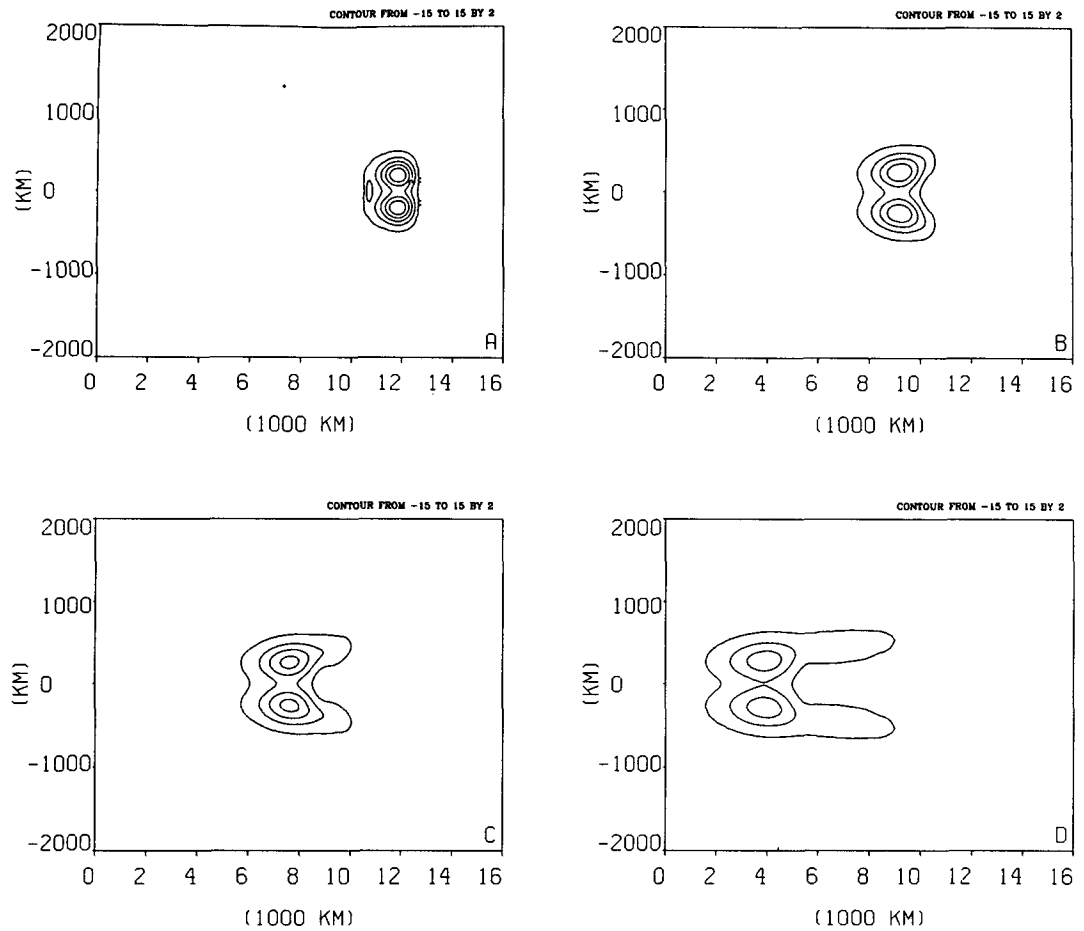

FIG. 3. Numerical simulations of long Rossby wave propagations at frequency $\omega = 2\pi/160$ days and $\delta = 1.25 \times 10^{-5}$ at (a) 150 days, (b) 250 days, (c) 325 days, and (d) 400 days.

wave. Figures 3a–d illustrate a propagating Rossby wave at $t = 150$, 250, 325, and 400 days, respectively, for $\delta = 1.25 \times 10^{-5}$ and wave frequency $\omega = 2\pi/160$ days. The wavelength of this westward long Rossby wave becomes longer when it propagates into the deeper western ocean. Its amplitude, however, reduces greatly to conserve its total energy. The numerical experiments are clearly consistent with the WKBJ solutions we derived in the previous section.

Now, consider a Kelvin wave impinging on a thermocline front where the MTD changes abruptly. The profile of the main thermocline is chosen so that it linearly changes from $H_0 = 200$ m to 100 m as x extends from 8500 km to 9500 km (see Fig. 4a). A Kelvin wave with a 100-day period is initiated at the western boundary and propagates into the interior ocean. Figure 4b displays the Kelvin wave at $t = 60$ days just when it hits the thermocline front. Wave reflection can be seen at $t = 80$ days (Fig. 4c). Figures 4d–e show the separation of this Kelvin wave and the reflected Rossby wave at $t = 100$ and 120 days, respectively. As we can see from these two pictures, most of the incoming Kelvin wave's energy is transmitted throughout the thermocline front for the chosen profile of the MTD. However, much more energy will be reflected if the thermocline front is steeper, or if the frequency of the wave is lower so that more Rossby wave modes are available.

5. Conclusion

By using the assumption that the change of the main thermocline depth is small in comparison with the wave amplitudes, we have derived the leading-order solutions of equatorially trapped waves. We also designed a simple reduced-gravity model to verify our analytical solutions and to test the effects of a steeper thermocline. Both analytical solutions and numerical simulations show that the wavelength of a Kelvin wave decreases while its amplitude increases to preserve its total energy when it propagates into an area of shallower thermocline depth. The short Rossby waves act in the opposite

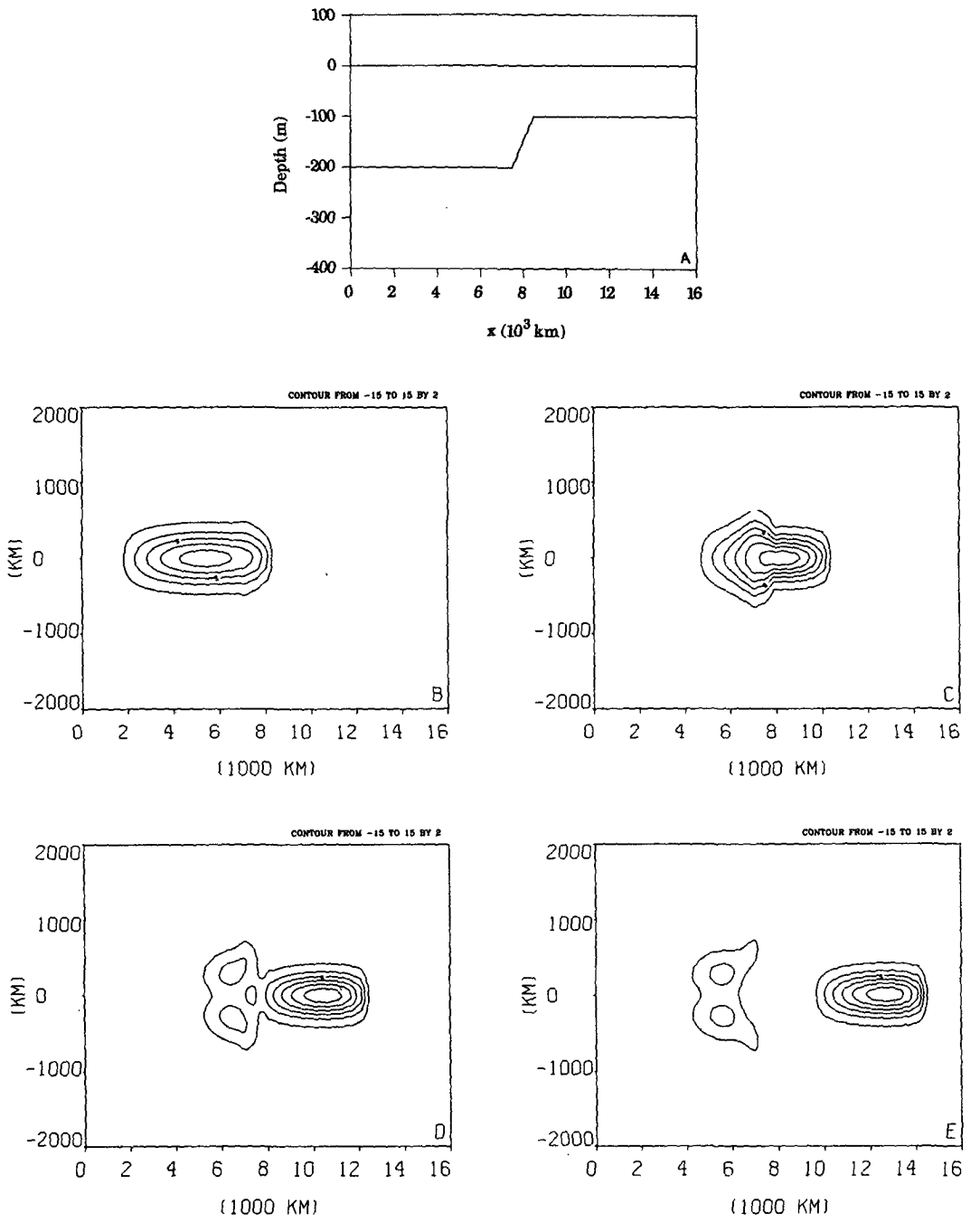

FIG. 4. Kelvin wave reflection at a thermocline front: (a) zonal cross section of the thermocline front and horizontal map (b) at 60 days, (c) at 80 days, (d) at 100 days, and (e) at 120 days.

way. For a long Rossby wave, its wavelength becomes longer when it travels to the deeper western ocean.

For an equatorially trapped Kelvin wave impinging on a steep thermocline front, part of its energy will be reflected as Rossby waves, while the remaining energy passes through the front and continues propagating eastward as a Kelvin wave.

Yanai waves also have significant responses to the sloping thermocline. The phase speed of a long Yanai wave with an initial westward phase speed may change in direction when the wave enters the shallower eastern ocean.

In conclusion, the linear wave solutions are significantly modified even when the depth of the main

equatorial thermocline varies slowly in the zonal direction, and so its effects should not be ignored in the tropical ocean models.

Acknowledgments. We deeply appreciate the encouragement, support, and guidance given by Dr. James J. O'Brien. Some helpful comments from Jorge Capella and Brian Kelly are acknowledged. We thank two anonymous reviewers for many helpful suggestions, especially for providing the references of Hughes (1981) and Gill and King (1985). This research is sponsored by the Physical Oceanographic Section of the National Science Foundation, the Oceanic Processes Branch of NASA and the Office of Naval Research. Lisan Yu is currently supported by the Florida State University Supercomputer Computations Institute, which is partially funded by the U.S. Department of Energy.

REFERENCES

Battisti, D. S., and A. C. Hirst, 1989: Interannual variability in a tropical atmosphere–ocean model: Influence of the basic state, ocean geometry and nonlinearity. *J. Atmos. Sci.*, **46,** 1687–1712.

Busalacchi, A. J., and J. J. O'Brien, 1980: The seasonal variability of the tropical Pacific. *J. Phys. Oceanogr.*, **10,** 1929–1952.

——, and M. A. Cane, 1988: The effects of varying stratification on low-frequency equatorial motions. *J. Phys. Oceanogr.*, **18,** 801–812.

Camerlengo, A. L., and J. J. O'Brien, 1980: Open boundary conditions in rotating fluids. *J. Comput. Phys.*, **35,** 12–35.

Cane, M. A., and Y. du Penhoat, 1981: The effects of islands on low frequency equatorial motions. *J. Mar. Res.*, **40,** 937–962.

Colin, C., C. Henin, P. Hisard, and C. Oudot, 1971: Le Courant de Cromwell dans le Pacifique central en février. *Cah. ORSTOM, Ser Oceanogr.*, **9,** 167–186.

Gill, A. E., and B. A. King, 1985: The effect of a shoaling thermocline on equatorial-trapped Kelvin waves. *Dynamical Climatology,* DCTN 27, 28 pp.

Hughes, T. L., 1981: The influence of thermocline slope on equatorial thermocline displacement. *Dyn. Atmos. Oceans,* **5,** 147–157.

Hurlburt, H. E., J. C. Kindle, and J. J. O'Brien, 1976: A numerical study of the onset of El Niño. *J. Phys. Oceanogr.*, **6,** 621–631.

Long, B., and P. Chang, 1990: On the propagation of an equatorial Kelvin wave in a varying thermocline. *J. Phys. Oceanogr.*, **20,** 1826–1841.

McCreary, J., 1976: Eastern tropical ocean response to changing wind system—with applications to El Niño. *J. Phys. Oceanogr.*, **6,** 632–645.

McPhaden, M. J., and J. Picaut, 1990: El Niño–Southern Oscillation displacements of the Western equatorial Pacific warm pool. *Science,* **250,** 1385–1388.

Merle, J., 1980: Seasonal heat budget in the equatorial Atlantic Ocean. *J. Phys. Oceanogr.*, **10,** 464–469.

Moore, D. W., 1968: Planetary–gravity waves in an equatorial ocean. Ph.D. thesis, Harvard University, 201 pp.

——, and S. G. H. Philander, 1977: Modeling of the tropical oceanic circulation. *The Sea, Vol. 6,* E. D. Goldberg, I. N. McCave, J. J. O'Brien, and J. H. Steel, Eds., Wiley-Interscience 319–361.

Philander, S. G. H., 1979: Equatorial waves in the presence of the Equatorial Undercurrent. *J. Phys. Oceanogr.*, **9,** 254–262.

Suarez, M. J., and P. S. Schopf, 1989: A delayed action oscillator for ENSO. *J. Atmos. Sci.*, **45,** 3283–3287.

Zebiak, S. E., and M. A. Cane, 1987: A model El Niño–Southern Oscillation. *Mon. Wea. Rev.*, **115,** 2262–2278.